OPEN ACCESS
IOP Publishing
Semiconductor Science and Technology
Semicond. Sci. Technol. **37** (2022) 105016 (8pp)
https://doi.org/10.1088/1361-6641/ac8e8f

Electrical properties and microstructure of V/Al/Ni/Au contacts on n-$Al_{0.65}Ga_{0.35}N$:Si with different Au thicknesses and annealing temperatures

H K Cho[1,*], A Mogilatenko[1], N Susilo[2], I Ostermay[1], S Seifert[1], T Wernicke[2], M Kneissl[1,2] and S Einfeldt[1]

[1] Ferdinand-Braun-Institut, Gustav-Kirchhoff-Str. 4, 12489 Berlin, Germany
[2] Technische Universität Berlin, Institute of Solid State Physics, Hardenberg-Str. 36, 10623 Berlin, Germany

E-mail: hyunkyong.cho@fbh-berlin.de

Received 12 May 2022, revised 8 August 2022
Accepted for publication 1 September 2022
Published 9 September 2022

Abstract

We investigated the formation of ohmic contacts as a result of intermetallic phase formation between V, Al, Ni, and Au in V/Al/Ni/Au metal stacks on n-$Al_{0.65}Ga_{0.35}N$:Si. In particular, the influence of Au metal thickness and annealing temperature was analysed. The lowest annealing temperature of 750 °C for an ohmic contact with a smooth surface and a contact resistivity of about 2.4×10^{-5} Ωcm^2 was achieved for V(15 nm)/Al(120 nm)/Ni(20 nm)/Au(40 nm). The lowest contact resistivity is accompanied by formation of two thin interfacial regions consisting of AlN and an Au-rich phase. We suggest that not only the formation of thin interfacial AlN layer is important for a low contact resistance, but also the formation of the Au-rich interface can have a favourable effect on the contact properties.

Keywords: ohmic contact, n-AlGaN, high Al mole fraction, UV LED, Au rich phase, AlN

(Some figures may appear in colour only in the online journal)

1. Introduction

Al-rich n-type AlGaN has been attracting significant attention because it is needed for ultraviolet light emitting diodes (UV LEDs) used for sterilization, water purification, and medical diagnostics [1, 2]. Hence, several efforts have been made to understand the contact formation mechanisms to Al-rich n-AlGaN in order to achieve low resistance contacts [3–10]. Concepts for ohmic contacts developed for n-GaN also work for Ga-rich n-AlGaN [11–13]. Here, Ti/Al-based metal stacks are typically used [14]. However, for Al-rich n-AlGaN, this type of contact is associated with a high potential barrier at the metal–AlGaN interface [15, 16] resulting in a significant nonlinearity of the current–voltage characteristics. As the Al mole fraction in n-AlGaN is increased, these contacts become more and more resistive and rectifying.

V/Al-based contacts were proposed for Al-rich AlGaN [4]. These contacts can be processed at a lower temperature and provide a lower contact resistance than Ti/Al-based contacts [8]. A thin nitride layer (typically VN or AlN) has been found to form at the corresponding metal–AlGaN interface [4, 8, 10]. Although not yet proven, it is nevertheless assumed that nitrogen atoms from AlGaN participate in the formation of this thin nitride layer, and that nitrogen vacancies created in AlGaN near the metal interface during this reaction act as donors. As

* Author to whom any correspondence should be addressed.

Original content from this work may be used under the terms of the Creative Commons Attribution 4.0 licence. Any further distribution of this work must maintain attribution to the author(s) and the title of the work, journal citation and DOI.

 © 2022 The Author(s). Published by IOP Publishing Ltd

a result, the increased donor concentration near the interface would reduce the width of the Schottky barrier and promote the tunneling of electrons. Up to now, V/Al-based metallizations with a Ni, Pd, Pt, or Mo diffusion barrier on top have been reported [4, 6]. A final Au cap layer is beneficial to reduce the sheet resistance of the contact and to limit oxidation [4, 8]. Besides that, it was found that the optimum V/Al thickness ratio is likely to be affected by the other elements (Ni or Au) present in the metal stack [8]. In addition, an increasing Al mole fraction in the AlGaN requires an increasing annealing temperature to achieve the lowest possible contact resistivity [9, 10].

While a number of chemical phases are known to form at the interface (VN, AlN, AlO_x, and Au) [8, 10], the reason for the ohmic behavior of a contact with an optimum V/Al thickness ratio, an optimum Au cap layer thickness, and an optimum annealing process is still unclear. Therefore, a more comprehensive analysis is required. Here, we present a study on the electrical and microstructural properties of V/Al/Ni/Au contacts with varying thickness of the Au cap layer annealed under different conditions.

2. Experimental

AlGaN heterostructures were grown by metal–organic vapour phase epitaxy (MOVPE) on *c*-plane sapphire substrates. First, a 500 nm thick AlN layer on sapphire was patterned into stripes by photolithography and dry etching and then epitaxially laterally overgrown by AlN to a total thickness of 6 μm [17]. Subsequently, a 900 nm thick $Al_{0.76}Ga_{0.24}N$:Si current spreading layer, a 100 nm $Al_{0.76}Ga_{0.24}N$:Si $\rightarrow$ $Al_{0.65}Ga_{0.35}N$:Si transition layer with gradually changing composition and a 500 nm $Al_{0.65}Ga_{0.35}N$:Si ($\sim 5 \times 10^{18}$ cm^{-3}) contact layer were grown [18]. The concentration of Si dopants in AlGaN was evaluated by secondary-ion mass spectrometry.

Test structures for determination of the specific contact resistance by the linear transmission line method (TLM) were fabricated by a lift-off process. First, 200 nm of the surface were etched using a mixture of BCl_3 and Cl_2 at a pressure of 1 Pa in an inductively coupled plasma-reactive ion etching system. An oxygen plasma was used to remove possible residues after photoresist development. Prior to the deposition of the n-contact metal stack, the plasma-etched surfaces were treated in HCl/H_2O (1:1) at room temperature for 30 s, rinsed in de-ionized water for 1 min and spin-dryed under nitrogen. Thereafter, two metal layer stacks with different Au thickness, i.e. V(15 nm)/Al(120 nm)/Ni(20 nm)/Au(20 nm) and V(15 nm)/Al(120 nm)/Ni(20 nm)/Au(40 nm), were deposited by electron-beam evaporation and structured by a lift-off process. The contacts were annealed at a maximum annealing temperature ranging from 700 °C to 850 °C in nitrogen ambient for 30 s using a rapid thermal annealing (RTA) furnace. Different annealing temperatures were tested on separate samples. Only the annealing at 850 °C was carried out after previous annealing at 800 °C. In addition, the heating speed

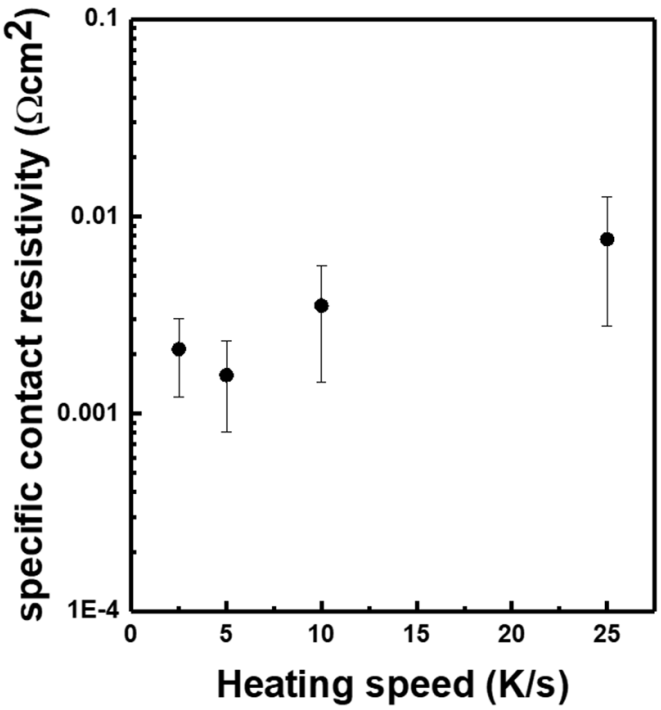

Figure 1. Specific contact resistivity of V(15 nm)/Al(120 nm)/Ni(20 nm)/Au(20 nm) contacts on n-$Al_{0.65}Ga_{0.35}N$:Si formed after annealing at 750 °C for 30 s using different heating speeds. Specific contact resistivities derived from TLM measurements at a current of 1 mA for the two metal systems.

was varied between 2.5 K s^{-1} and 25 K s^{-1}. The contacts had a size of 460 μm $\times$ 100 μm and spacings of 10 μm, 15 μm, 20 μm, 25 μm, and 30 μm, respectively. Current–voltage (*I*–*V*) measurements were performed at room temperature.

The surface morphology of the metal contacts was examined by scanning electron microscopy (SEM). Cross-section transmission electron microscopy (TEM) samples were prepared to examine the phase formation in the metal layer stack after annealing. High resolution TEM (HRTEM) using broad parallel beam illumination and high angle annular dark-field scanning TEM (HAADF STEM) in combination with energy dispersive x-ray (EDX) spectroscopy and electron energy loss spectroscopy (EELS) were performed to reveal the structure and the compositional uniformity of the metal–semiconductor interface.

3. Results and discussion

Figure 1 shows the specific contact resistivity of V(15 nm)/Al(120 nm)/Ni(20 nm)/Au(20 nm) contacts obtained for different temperature ramp rates from room temperature to the maximum temperature of 750 °C. The lowest contact resistivities are obtained for the slowest temperature ramp rates of 2.5 K s^{-1} and 5 K s^{-1}. This indicates that for a low contact resistivity, diffusion processes (presumably of the contact metals) must take place to a sufficient extent. This is only given if the time available for diffusion is long enough,

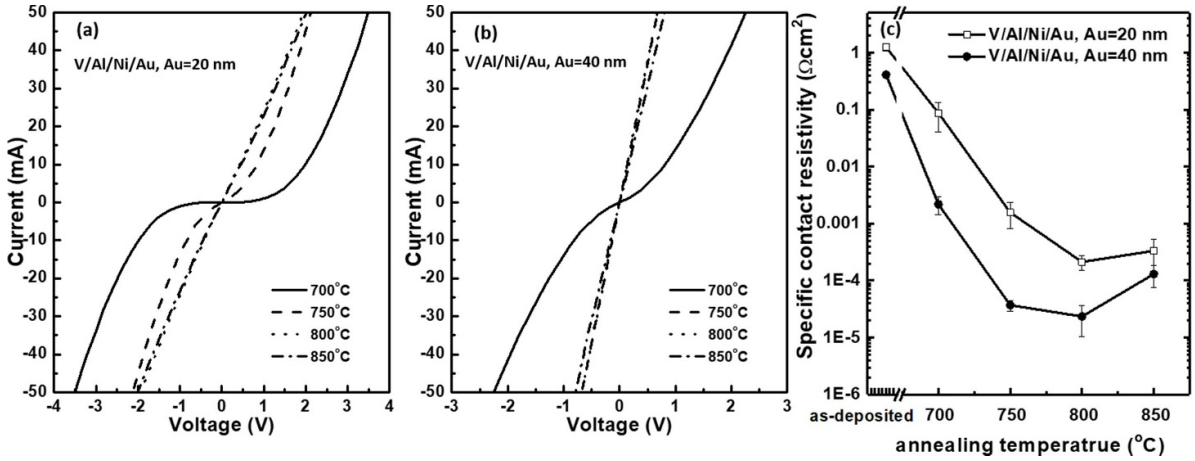

Figure 2. *I–V* curves from two-point measurements between contacts of 20 μm distance on n-$Al_{0.65}Ga_{0.35}N$:Si obtained after annealing at different temperatures (a) V(15 nm)/Al(120 nm)/Ni(20 nm)/Au(20 nm), and (b) V(15 nm)/Al(120 nm)/Ni(20 nm)/Au(40 nm). (c) Specific contact resistivities derived from TLM measurements at a current of 1 mA for the two metal systems.

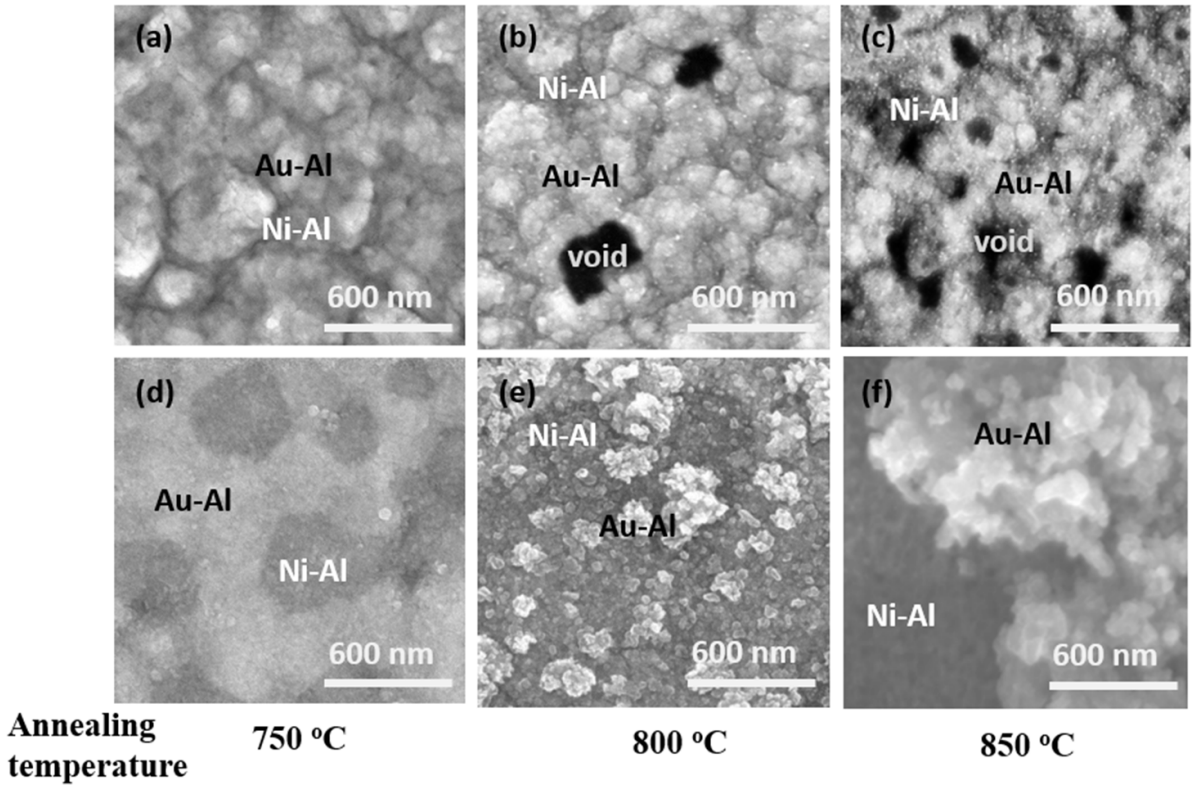

Figure 3. Top-view SEM images of metal contacts on $Al_{0.65}Ga_{0.35}N$:Si annealed at different temperatures: (a)–(c) V(15 nm)/Al(120 nm)/Ni(20 nm)/Au(20 nm), and (d)–(f) V(15 nm)/Al(120 nm)/Ni(20 nm)/Au(40 nm).

i.e. here if the ramp rate is small enough. Therefore, all following annealing experiments have been performed with a heating speed of 5 K s^{-1}.

Figures 2(a) and (b) show the *I–V* curves of the two types of contacts for different maximum annealing temperatures. Also, the corresponding specific contact resistivities derived from TLM measurements are shown in figure 2(c). The as-deposited contacts (not shown here) are rectifying. By increasing the annealing temperature, the *I–V* characteristics become linear after annealing beyond 800 °C (figure 2(a)) and 750 °C (figure 2(b)), respectively. A minimum specific contact resistivity is reached around 800 °C for both Au thicknesses, i.e. 2.1×10^{-4} Ωcm^2 and 2.4×10^{-5} Ωcm^2, for a Au thickness of 20 nm and 40 nm, respectively.

The morphology and composition of the contact surfaces was studied by SEM (figure 3) and EDX (figures 4 and 5). Figure 3 shows the comparison of the surface morphology of the two sets of samples (with 20 nm and 40 nm Au cap layer)

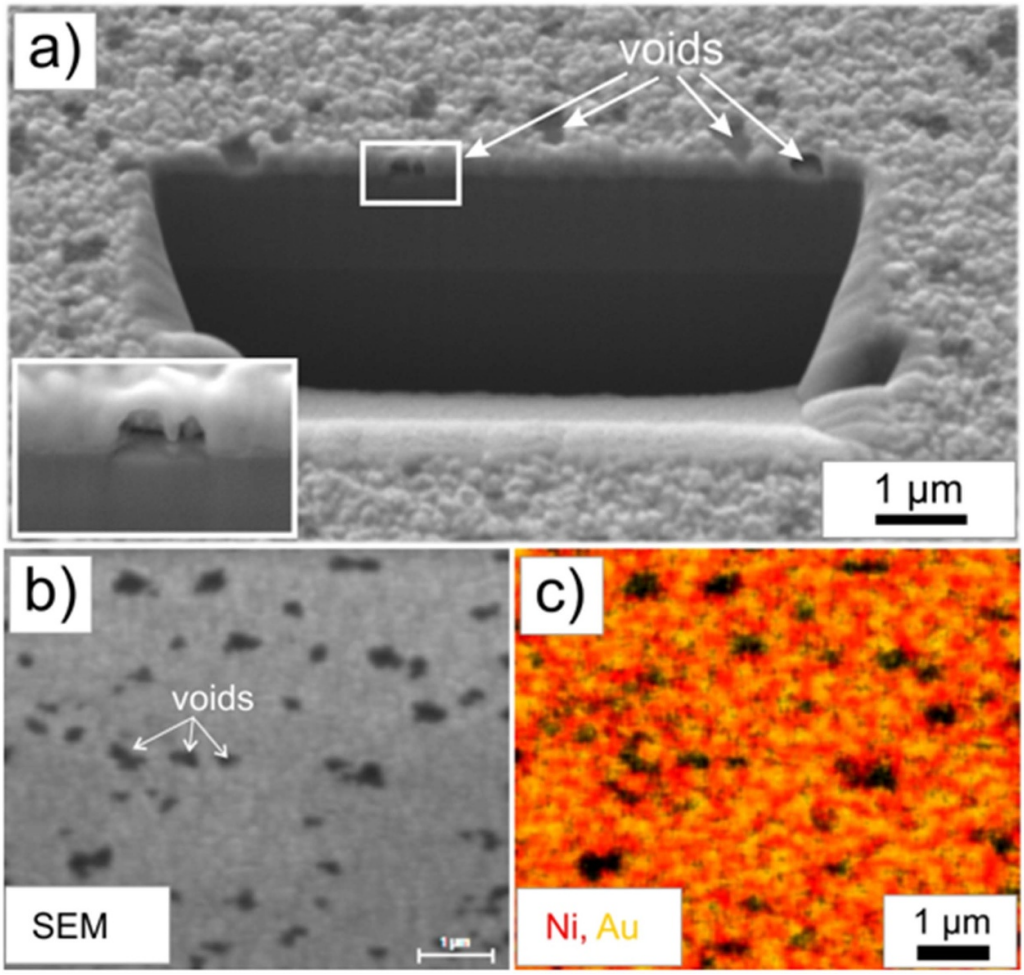

Figure 4. (a) SEM bird's eye view of a FIB cut in a V(15 nm)/Al(120 nm)/Ni(20 nm)/Au(20 nm) contact after annealing at 850 °C (inset in the lower corner shows a magnified image of a void in the layer); (b) top-view SEM image (b) and corresponding EDX map (c) showing the distribution of Au-M and Ni-L peak intensities (V-K and Al-K maps showed a uniform intensity distribution and thus are not shown here).

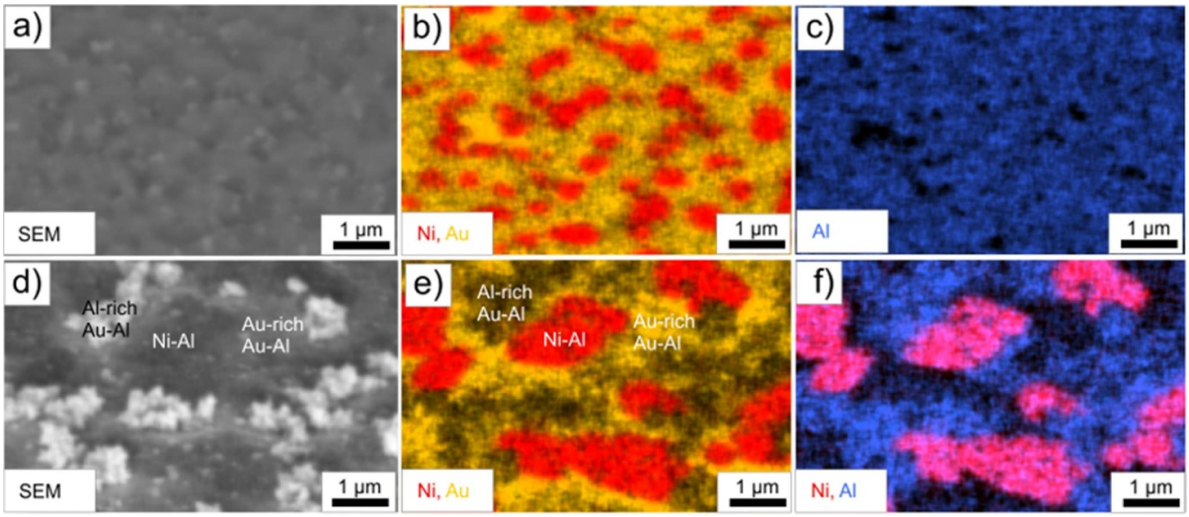

Figure 5. Top-view SEM images (a), (d) and EDX maps (b), (c), (e), (f) acquired at V(15 nm)/Al(120 nm)/Ni(20 nm)/Au(40 nm) contacts after annealing at 750 °C (a)–(c) and 850 °C (d)–(f), respectively.

after annealing at different temperatures. Up to an annealing temperature of 750 °C, the surface of both metallization stacks remains relatively smooth (figures 3(a) and (d)). However, when further increasing the annealing temperature up to 850 °C, the surface morphology changes. For the 20 nm thick Au cap layer voids are formed at 800 °C. Their number increases with increasing annealing temperature, as shown in figures 3(b) and (c). In particular, focused ion beam (FIB) was used to prove the formation of voids in the contact layers after annealing at 850 °C (figure 4(a)). EDX maps show a uniform distribution of small grains in this sample which correspond to two phases: Ni–Al and Au–Al (for Au and Ni signal see figure 4(c), the Al and V signals were uniformly distributed and thus are not shown here). Obviously, for a Au cap layer thickness of 20 nm elevated annealing temperatures promote the formation of voids.

In contrast, with increasing annealing temperature the contact with the 40 nm thick Au cap layer shows an enhanced formation of bumps of irregular shape protruding from the surface (figures 3(e) and (f)). The lateral size and the height of these bumps increase with increasing annealing temperature further. According to EDX analysis, there are grains of different sizes and random distribution, which correspond to phases of Ni–Al and Au–Al (figure 5). This is similar to the contact with the 20 nm thick Au cap layer discussed before. However, the grain size distribution of these phases changes with increasing annealing temperature (figure 5). After annealing at 750 °C small Ni–Al grains with a lateral size up to 500 nm have formed which are surrounded by a matrix of an Au–Al alloy (figures 5(a)–(c)). For a higher annealing temperature of 850 °C, the Ni–Al grain size increases up to a few micrometres (figure 5(e)). Simultaneously, there is a phase separation of the Au–Al phase into Au-rich and Al-rich phases (figures 5(e) and (f)). Note that the formation of bumps on the surface is a consequence of this phase separation, because the Al-rich Au–Al regions protrude from the surface (compare figures 5(d) and (e)).

In general, Au is used as a cap layer to protect V and Al from oxidation during the RTA process [3]. In addition, a diffusion barrier layer (Ti or Ni) is typically used [6, 7] below the Au cap layer to suppress Au from fast diffusion to the AlGaN interface. In reality, however, a strong intermixing of all involved metals takes place at high annealing temperatures. It was shown, that the surface of Ti/Al/Ni/Au contacts roughens at high annealing temperature due to balling up of melted Al or the formation of AlNi, Al_2Au, and $AlAu_4$ phases [7, 19–21]. We assume that a similar process takes place for our V/Al/Ni/Au contacts when the Au cap layer is 40 nm thick.

The reaction between Al and Au that takes place during annealing is expected to be governed mainly by the diffusion of Au, which is much faster than that of Al [22]. It is likely that it is these large differences in diffusion coefficients that result in Au vacancies and their agglomeration into voids (Kirkendall effect) [23, 24]. Moreover, the formation of Au–Al phases is accompanied by a change in density and thus a change in volume. While for the Au-rich phases AuAl and Au_2Al the volume decreases, it increases for the Al-rich phase $AuAl_2$ [21]. Due to the preferential diffusion of the Au, Au-rich Au–Al phases are probably formed first in the upper part of the metal layer stack, which is accompanied by a reduction in volume and the formation of voids (compare sample with 20 nm thin Au cap layer). The Al-rich Au–Al phases with larger volume can form later in the lower part of the metal layer stack only if sufficient Au is available. This would be consistent with the observation of Al-rich Au–Al bumps on the surface of the sample with the 40 nm thick Au cap layer.

The microstructure of the annealed contacts was further investigated by TEM. Figure 6 shows TEM images of the V(15 nm)/Al(120 nm)/Ni(20 nm)/Au(40 nm) contact annealed at 750 °C. According to EDX analysis Au–Al, Ni–Al and V–Al–Au phases have been formed as separate grains. Ni–Al and Au–Al metal phases were also observed by SEM-based EDX on the top surface of the contact, as shown in figure 3(d). Similar phases were observed for V/Al/Ni/Au contacts on n-$Al_{0.75}Ga_{0.25}N$:Si by Sulmoni *et al* [10]. Note that these phases are not in direct contact with the n-$Al_{0.65}Ga_{0.35}N$:Si surface. The HRTEM images in figures 6(b)–(d) show three discontinuous regions with different thin interlayers at the metal/semiconductor interface:

(a) A few monolayers thick crystalline AlN layer which appears bright in HRTEM images (figure 6(b)) and dark in HAADF STEM images (figure 6(e)) due its low mean atomic number.
(b) An amorphous AlON layer which appears bright in HRTEM images (see figure 6(c) and EELS spectrum in figure 6(f) with the simultaneous presence of O and N).
(c) An Au-rich region, which appears dark in HRTEM images (figure 6(d)).

The formation of the thin AlN interlayer is believed to result from the diffusion of Al out of the metal stack through the V layer to the AlGaN surface accompanied by N out-diffusion from the AlGaN [10]. This process would deplete the AlGaN of nitrogen, i.e. nitrogen vacancies would form which should be donors in AlGaN. An increased donor concentration would thin the Schottky barrier at the interface and reduce the contact resistance [24, 25]. The importance of the formation of an AlN layer at the interface for a low specific contact resistance has been discussed before [8, 10]. The formation of AlN at the interface seems plausible in that the binding energy of AlN is greater than that of VN and GaN [26, 27].

On the other hand, the simultaneous presence of AlON regions suggests that oxide residues may have remained on the n-AlGaN:Si surface prior to metal deposition—possibly from the oxygen plasma treatment. Also, the formation of three different interfacial regions was also reported for annealed V/Al/Ni/Au contacts on n-$Al_{0.75}Ga_{0.25}N$:Si [10], with the authors focusing on the formation of AlN and AlON. It should be noted that n-type GaN or AlGaN with low Al content are often treated by oxygen plasma prior to metallization to increase the carrier concentration at the surface and form a tunnelling contact [28, 29]. However, for AlGaN with high Al content, this approach seems to be disadvantageous. Vacancies

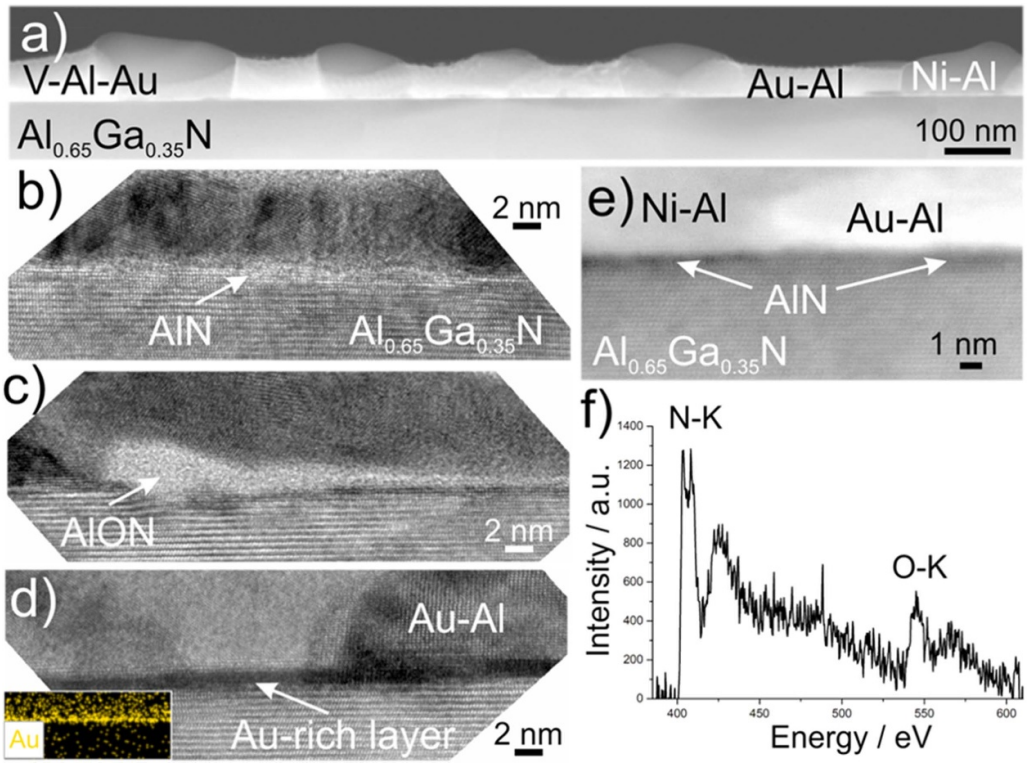

Figure 6. (a) Exemplary HAADF STEM image of the V(15 nm)/Al(120 nm)/Ni(20 nm)/Au(40 nm) contact annealed at 750 °C; (b)–(d) HRTEM images showing three different interfacial regions simultaneously present in the sample; the inset in (d) is an EDX map showing the distribution of the Au-L peak intensity; (e) HAADF STEM image showing an a few monolayers thick interfacial AlN layer appearing dark in the image; (f) EELS spectrum obtained using a beam size of 1 nm in the interfacial region shown in (c).

and incorporated oxygen from plasma etching are believed to form acceptor-like states, compensate the n-doping and thus degrade the contact resistance [30]. Besides, in an earlier work, we found that aluminum oxide or oxynitride forms at the surface of Al-rich n-AlGaN during oxygen plasma treatment which can hardly be removed by subsequent wet-chemical surface treatment [9]. In this context, it should also be mentioned, that it is unclear how the Au-rich regions at the interface (see figure 6(d)) influence the electrical properties of the contact.

TEM-based EDX investigations of the contact with the thinner Au cap layer of 20 nm annealed at 850 °C provide less reliable data due to the smaller grains, which lead to projection effects, i.e. a number of grains with different compositions are simultaneously probed in the thin specimen prepared for cross-sectional TEM. This results in an EDX signal averaging over different grains and thus different phases. For the 20 nm thick Au layer, Ni–Al and Ni–Au–Al phases were observed after annealing at 850 °C (figure 7(a)). Binary Au–Al phases were not found in this sample, probably as a result of the low Au amount in the metal stack. However, the aforementioned projection effect may have prevented existing Au–Al and Ni–Al grains from being detected separately.

Similarly, to the sample with 40 nm thick Au layer, the formation of thin AlN and AlON was revealed at the interface to AlGaN for the sample with 20 nm thick Au as well. However, two distinct differences compared to the sample with the 40 nm thick Au cap layer were found: (a) the presence of V–Al grains instead of V–Al–Au close to the AlGaN interface, and (b) the absence of Au-rich regions at the metal/semiconductor interface (note the bright Au rich layer in figure 7(b) and its absence in figure 7(a)). Both findings can be attributed to the lack of Au participating in the solid phase reaction during annealing, which prevents the formation of Au-rich phases. The presence of Au-rich regions at the semiconductor interface as in our sample with the 40 nm thick Au cap layer has also been observed by others, e.g. for annealed Ti/Al/Ni/Au contacts on n-$Al_{0.28}Ga_{0.72}N$ [7]. In this case these regions occurred in the sample with the lowest contact resistivity. Therefore, one can speculate that Au-rich regions may actually be important to ensure that the lowest contact resistivity possible is achieved.

Combining the observed structural differences and the measured electrical properties, suggests that not only the formation of a thin interfacial AlN layer at the metal/AlGaN interface, but also the Au cap layer thickness and the subsequent formation of Au-rich regions at the metal/AlGaN interface (figures 6(d) and 7(b)) have an important influence on the contact properties. Furthermore, the apparent increase in roughness and discontinuity in the ohmic metal contact due to the formation of Au–Al phases may affect the specific contact resistivity. As shown in figure 2(c), the contact resistivity of the sample with V(15 nm)/Al(120 nm)/Ni(20 nm)/Au(20 nm) does not change when increasing the annealing temperature from 800 °C to 850 °C and it is always higher than

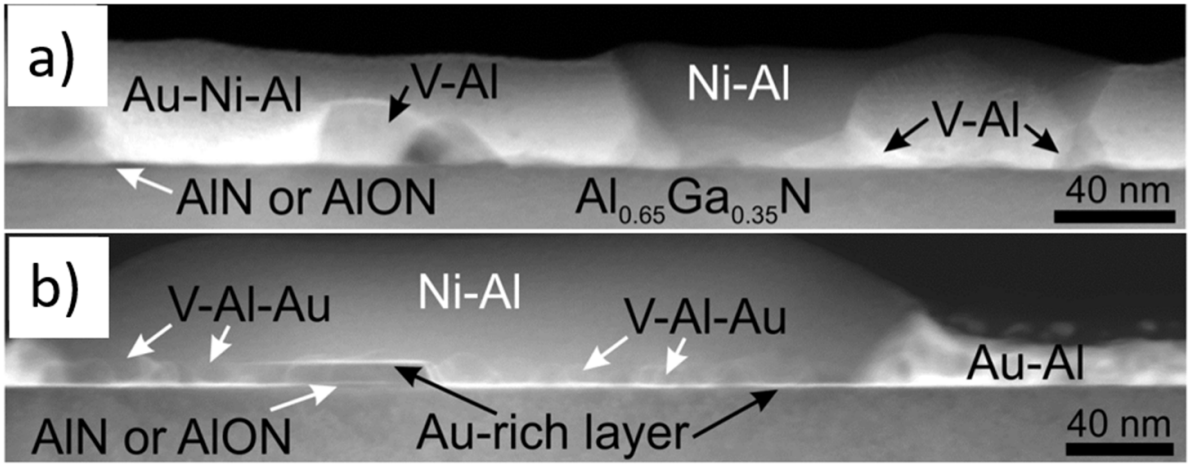

Figure 7. HAADF STEM images summarizing phases detected using EDX in (a) V(15 nm)/Al(120 nm)/Ni(20 nm)/Au(20 nm) contact annealed at 850 °C and (b) V(15 nm)/Al(120 nm)/Ni(20 nm)/Au(40 nm) contact annealed at 750 °C.

those of the samples with 40 nm Au. We attribute, the higher contact resistivity values observed for 20 nm thick Au cap layer to the lack of Au-rich phases after high temperature annealing.

In our work, the influence of Au thickness as well as annealing temperature on the formation of low-resistance V/Al/Ni/Au contacts were tested using Al-rich n-AlGaN. Generally speaking, the results support the well-known fact that the design of the metal layer stack as well as the annealing conditions are important to obtain a beneficial reaction between the metals and the semiconductor. However, due to the complexity of the reaction processes, iterative empirical variations will always be necessary to find the technology optimum.

4. Summary

The electrical and microstructural properties of V/Al/Ni/Au contacts with different Au cap layer thicknesses on n-$Al_{0.65}Ga_{0.35}N$:Si were investigated. A reasonably low specific contact resistivity of 2.4×10^{-5} Ωcm^2 and a smooth contact surface were achieved for the V(15 nm)/Al(120 nm)/Ni(20 nm)/Au(40 nm) layer system annealed at the lowest annealing temperature of 750 °C. The achievement of a low-resistance ohmic contact is facilitated by the formation of intermetallic phases of Ni, Al, V, and Au at different annealing temperatures. We found that a low contact resistance is accompanied by formation of interfacial AlN as well as Au-rich layers. Thus, we suggest that a sufficiently thick Au cap layer and an optimal annealing temperature play a crucial role for both a smooth surface morphology of the contact and a low contact resistance. We anticipate that these findings will help to further reduce the operating voltages of AlGaN-based devices, e.g. UVC-LEDs.

Data availability statement

No new data were created or analysed in this study.

Acknowledgments

The authors would like to thank the Process Technology Department at the Ferdinand-Braun-Institut in general for their contributions to the developments of contacts for UV LEDs as well as Helen Lawrenz for preparation of FIB cross-sections samples and acquisition of EDX-maps in SEM. We thank Praphat Sonka for operation of the MOVPE system at TU Berlin. This work was partially supported by the German Federal Ministry of Education and Research (BMBF) in the 'Advanced UV for Life' consortium under Contracts 03ZZ0134B and 03ZZ0134C.

ORCID iDs

H K Cho https://orcid.org/0000-0001-5540-2582
N Susilo https://orcid.org/0000-0002-5583-629X
M Kneissl https://orcid.org/0000-0003-1476-598X
S Einfeldt https://orcid.org/0000-0001-7502-7812

References

[1] Hirayama H 2005 Quaternary InAlGaN-based high-efficiency ultraviolet light-emitting diodes *J. Appl. Phys.* **97** 091101
[2] Kneissl M and Rass J (eds) 2016 *III-Nitride Ultraviolet Emitters—Technology & Applications* (*Series on Material Science* vol 227) (Berlin: Springer)
[3] van Daele B, van Tendeloo G, Ruythooren W, Derluyn J, Leys M R and Germain M 2005 The role of Al on ohmic contact formation on n-type GaN and AlGaN/GaN *Appl. Phys. Lett.* **87** 061905
[4] Wang J, Mohney S E, Wang S H, Chowdhury U and Dupuis R D 2004 Vanadium-based ohmic contacts to n-type $Al_{0.6}Ga_{0.4}N$ *J. Electron. Mater.* **33** 1
[5] Readinger E D, Mohney S E, Pribicko T G, Wang J H, Schweitz K O, Chowdhury U, Wong M M, Dupuis R D, Pophristic M and Guo S P 2002 Ohmic contacts to Al-rich n-AlGaN *Electron. Lett.* **38** 1230
[6] Miller M A, Koo B H, Bogart K H A and Mohney S E 2008 Ti/Al/Ti/Au and V/Al/V/Au contacts to plasma-etched n-$Al_{0.58}Ga_{0.42}N$ *J. Electron. Mater.* **37** 564

[7] Brigit A N, Thomas P J, Weyland M, Tricker D M, Humphreys C J and Davies R 2001 Correlation of contact resistance with microstructure for Au/Ni/Al/Ti/AlGaN/GaN ohmic contacts using transmission electron microscopy *J. Appl. Phys.* **89** 3143

[8] Schmid A, Schroeter C, Otto R, Schuster M, Klemm V, Rafaja D and Heitmann J 2015 Microstructure of V-based ohmic contacts to AlGaN/GaN heterostructures at a reduced annealing temperature *Appl. Phys. Lett.* **106** 053509

[9] Lapeyrade M *et al* 2017 Effect of Cl_2 plasma treatment and annealing on vanadium-based metal contacts to Si-doped $Al_{0.75}Ga_{0.25}N$ *J. Appl. Phys.* **122** 125701

[10] Sulmoni L, Mehnke F, Mogilatenko A, Guttmann M, Wernicke T and Kneissl M 2020 Electrical properties and microstructure formation of V/Al-based n-contacts on high Al mole fraction n-AlGaN layers *Photon. Res.* **8** 1381

[11] Lui Q Z, Yu L S, Deng F, Lau S S, Chen Q, Yang J W and Khan M A 1997 Study of contact formation in AlGaN/GaN heterostructures *Appl. Phys. Lett.* **71** 1658

[12] Ruvimov S, Liliental-Weber Y, Washburn J, Qiao D, Lau S S and Chu Paul K 1998 Microstructure of Ti/Al ohmic contacts for n-AlGaN *Appl. Phys. Lett.* **73** 2582

[13] Greco G, Iucolano F and Roccaforte F 2016 Ohmic contacts to gallium nitride materials *Appl. Surf. Sci.* **383** 324

[14] Kim J K, Jang H W and Lee J L 2002 Mechanism for ohmic contact formation of Ti on n-type GaN investigated using synchrotron radiation photoemission spectroscopy *J. Appl. Phys.* **91** 9214

[15] Reddy P, Bryan I, Bryan Z, Guo W, Hussey L, Collazo R and Sitar Z 2014 The effect of polarity and surface states on the Fermi level at III-nitride surfaces *J. Appl. Phys.* **116** 123701

[16] Binari S C and Dietrich H B 1997 *III–V Nitride Electronic Devices, in GaN and Related Materials* vol 2 (Boca Raton, FL: CRC Press)

[17] Kueller V, Knauer A, Zeimer U, Rodriguez H, Mofilatenki A, Keissl M and Weyers M 2011 (Al, Ga)N overgrowth over AlN ridges oriented in [1120] and [1100] direction *Phys. Status Solidi* c **8** 2022

[18] Susilo N *et al* 2020 Improved performance of UVC-LEDs by combination of high-temperature annealing and epitaxially laterally overgrown AlN/sapphire *Photon. Res.* **8** 589

[19] Gong R, Wang J, Liu S, Dong Z, Yu M, Wen C P, Cai Y and Zhang B 2010 Analysis of surface roughness in Ti/Al/Ni/Au ohmic contact to AlGaN/GaN high electron mobility transistors *Appl. Phys. Lett.* **97** 062115

[20] Roccaforte F, Iucolano F, Giannazzo F, Alberti A and Raineri V 2006 Nanoscale carrier transport in ohmic contacts on AlGaN epilayers grown on Si(111) *Appl. Phys. Lett.* **89** 022103

[21] Wang L, Mohammed F M and Adesida I 2008 Formation mechanism of ohmic contacts on AlGaN/GaN heterostructure: electrical and microstructural characterizations *J. Appl. Phys.* **103** 093516

[22] Xu H, Liu C, Silberschmidt V V, Pramana S S, White T J, Chenc Z and Acof V L 2011 New mechanisms of void growth in Au–Al wire bonds: volumetric shrinkage and intermetallic oxidation *Scr. Mater.* **65** 642

[23] Xu C, Sritharan T and Mhaisalkar S G 2007 Interface transformations in thin film aluminum–gold diffusion couples *Thin Solid Films* **515** 5454

[24] Perlin P *et al* 1995 Towards the identification of the dominant donor in GaN *Phys. Rev. Lett.* **75** 296

[25] Stampfl C and van de Walle C G 2002 Theoretical investigation of native defects, impurities, and complexes in aluminum nitride *Phys. Rev.* B **65** 155212

[26] Dronskowski R 2017 *Handbook of Solid State Chemistry* vol 6 (Weinheim: Wiley)

[27] Schweitz K O and Mohnex S E 2001 Phase equilibria in transition metal Al-Ga-N systems and thermal stability of contacts to AlGaN *J. Electron. Mater.* **30** 175

[28] Yan J, Kappers M J, Berber Z H and Humphreys C J 2004 Effects of oxygen plasma treatments on the formation of ohmic contacts to GaN, and complexes in aluminum *Appl. Surf. Sci.* **234** 328

[29] Seo H, Cha Y-J, Mohammad A B, Islam H and Kwak J S 2020 Improvement of Ti/Al ohmic contacts on N-face n-type GaN by using O_2 plasma treatment *Appl. Surf. Sci.* **510** 145180

[30] Zhang N *et al* 2021 Improved ohmic contacts to plasma etched high Al fraction n-AlGaN by active surface pretreatment *Appl. Phys. Lett.* **118** 222101